

OVERLAY COGNITIVE RADIO USING SYMBOL LEVEL PRECODING WITH QUANTIZED CSI

Lu Liu and A. Lee Swindlehurst

Center for Pervasive Communications & Computing, University of California, Irvine, CA, USA

ABSTRACT

Overlay cognitive radio (CR) networks include a primary and cognitive base station (BS) sharing the same frequency band. This paper focuses on designing a robust symbol-level precoding (SLP) scheme where the primary BS shares data and quantized channel state information (CSI) with the cognitive BS. The proposed approach minimizes the cognitive BS transmission power under symbol-wise Safety Margin (SM) constraints for both the primary and cognitive systems. We apply the additive quantization noise model to describe the statistics of the quantized PBS CSI and employ a stochastic constraint to formulate the optimization problem, which is then converted to be deterministic. Simulation results show that the robust SLP protects the primary users from the effect of the imperfect CSI and simultaneously offers significantly improved energy efficiency compared to non-robust methods.

Index Terms— cognitive radio, symbol-level precoding, constructive interference, robust precoding, quantization.

1. INTRODUCTION

Cognitive radio (CR) systems must balance the interference produced at the primary users (PUs) with the quality of service (QoS) provided to the cognitive users (CUs) [1–3]. In this paper, we employ symbol level precoding (SLP) to address this issue. Instead of treating interference as a source of degradation, SLP instead exploits it as a potential resource to improve performance. SLP uses information about the transmit symbols in addition to the channel state information (CSI) to provide additional degrees of freedom that converts multi-user interference into constructive interference (CI), moving the received signals further from the symbol decision thresholds [4,5]. CI-based SLP approaches are intended to increase the distance or “Safety Margin” (SM) of the constructive interference regions (CIRs) from the symbol decision boundaries to improve the symbol error rate [6–9]. Ideally, the SM should be large enough to control the probability that noise or other impairments will push the noise-free signal outside the detection region; the larger the SM, the smaller the SER.

This work was supported by the National Science Foundation under grants CCF-2008714 and CCF-2225575.

The performance of SLP is sensitive to imprecise CSI due for example to errors introduced by channel estimation, quantization, or latency-related effects [10–12]. Depending on the SM, the imperfect CSI may even cause the noise-free received symbols to fall outside the desired CIR. Consequently, robust designs are needed that properly model the CSI and allow for more intelligent CIR design. While robust designs for traditional MIMO or CR scenarios have been investigated [13–16], robust SLP schemes for CR have not. Prior work on robust designs for SLP includes [6], which derived an SLP algorithm suitable for imperfect CSI with bounded CSI errors, but it is based on a multicast formulation that does not take full advantage of the CI. The work described in [17, 18] considered a linear channel distortion model with bounded additive noise and Gaussian-distributed channel uncertainties. They designed robust SLP algorithms to minimize transmit power subject to both CI and SINR constraints. While not focused on CR, this prior work demonstrates that robust SLP designs can be formulated to achieve a better balance between performance and power consumption.

In this paper, we propose a robust CR SLP approach for a CSI error model that accounts for quantization in the CSI shared by the PBS. In particular, we focus on overlay CR channels [2, 3] where the PBS shares with the CBS its quantized CSI for the PUs and CUs, as well as its data intended for the PUs. We use the additive quantization noise model (AQNM) [19,20] to describe the quantization error, which has been widely used in the analysis of quantized MIMO systems. We formulate the problem of minimizing the CBS transmit power while simultaneously satisfying SM constraints at both the PUs and CUs within a certain probability. Then, we apply the *Safe Approximation I* method in [18] to reformulate the intractable probabilistic constraints as deterministic constraints. To validate the effectiveness of our proposed robust precoders, we conduct simulations assuming the PBS channel is quantized using the scalar Lloyd Max algorithm which minimizes the average quantization noise power.

2. SYSTEM MODEL AND SLP

We consider a downlink CR network with an M_c -antenna CBS serving N_c single-antenna CUs. The CBS shares the primary system spectrum in which an M_p -antenna PBS is com-

municating with N_p single-antenna PUs, as depicted in Fig. 1. The direct primary and cognitive channels are respectively denoted by the flat-fading models $\mathbf{H}_{pp} = [\mathbf{h}_{pp,1}^T \cdots \mathbf{h}_{pp,N_p}^T]^T$ and $\mathbf{H}_{cc} = [\mathbf{h}_{cc,1}^T \cdots \mathbf{h}_{cc,N_p}^T]^T$. The corresponding interference channels are defined as $\mathbf{H}_{pc} = [\mathbf{h}_{pc,1}^T \cdots \mathbf{h}_{pc,N_p}^T]^T$ and $\mathbf{H}_{cp} = [\mathbf{h}_{cp,1}^T \cdots \mathbf{h}_{cp,N_p}^T]^T$, from the PBS to CUs and the CBS to PUs, respectively.

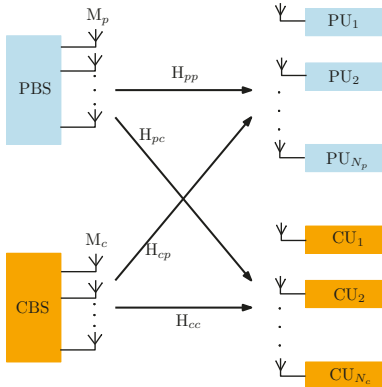


Fig. 1. Cognitive Radio System Model

The vectors $\mathbf{s}_p = [s_{p,1} \ s_{p,2} \ \cdots \ s_{p,N_p}]^T$ and $\mathbf{s}_c = [s_{c,1} \ s_{c,2} \ \cdots \ s_{c,N_c}]^T$ contain the modulated signals to be transmitted to the individual PUs and CUs. In this work we assume for simplicity that all transmitted symbols are uncorrelated and drawn from a D -PSK constellation with unit magnitude, i.e., $s_{l,m} \in \{s | s = \exp(j\pi(2d+1))/D, d \in \{0, \dots, D-1\}\}$ where $l \in \{p, c\}$ denotes the primary or cognitive system, and m denotes the user index in the corresponding system. The sets $\mathcal{K} = \{1, \dots, N_p\}$ and $\mathcal{J} = \{1, \dots, N_c\}$ enumerate the PUs and CUs, respectively. The idea of CI precoding can in principle be applied to any constellation design [8], e.g., QAM or otherwise, but is most easily formulated for the case of PSK signals. The received signals at the PUs and CUs can be respectively written as

$$\mathbf{y}_p = \mathbf{H}_{pp}\mathbf{x}_p + \mathbf{H}_{cp}\mathbf{x}_c + \mathbf{n}_p \quad (1)$$

$$\mathbf{y}_c = \mathbf{H}_{cc}\mathbf{x}_c + \mathbf{H}_{pc}\mathbf{x}_p + \mathbf{n}_c \quad (2)$$

where $\mathbf{x}_p \in \mathbb{C}^{M_p \times 1}$ and $\mathbf{x}_c \in \mathbb{C}^{M_c \times 1}$ are the transmitted signals at the PBS and CBS after precoding and power loading, and $\mathbf{n}_p \sim \mathcal{CN}(0, \sigma_p^2 \mathbf{I})$ and $\mathbf{n}_c \sim \mathcal{CN}(0, \sigma_c^2 \mathbf{I})$ are additive white Gaussian noise (AWGN) vectors.

For PSK constellations, it is not necessary that a given user's noise-free received signal $r_m = \mathbf{h}_m \mathbf{x}$ be close to its corresponding constellation point s_m in order to be decoded correctly, as long as it lies in the correct decision region with a given level of certainty. Thus, it is not necessary that all of the inter-user interference be eliminated, since some interference components could add constructively and push the received symbol further into the decision region, making it more robust

to noise and interference external to the system. Following the approach of [7], we rotate the noise-free received signal by the phase of the desired constellation symbol, $\angle s_m$, to obtain $z_m = r_m s_m^*$, in which case the SM δ_m for user m can be defined as

$$\delta_m = \mathcal{R}\{z_m\} \sin \theta - |\mathcal{I}\{z_m\}| \cos \theta, \quad (3)$$

where $\mathcal{R}\{\cdot\}$ and $\mathcal{I}\{\cdot\}$ respectively denote the real and imaginary part of a complex number.

3. POWER MINIMIZATION SLP IN CR

We first examine the case where the PBS shares its data and *perfect* CSI with the CBS. The SM for the PUs and CUs is constrained to be at least δ_p^0 and δ_c^0 , and we focus on SLP designs that minimize the transmit power at the CBS subject to the SM constraints.

The rotated symbols at the PUs can be expressed as

$$z_{p,k} = s_{p,k}^* r_{p,k} = \tilde{\mathbf{h}}_{pp,k} \mathbf{x}_p + \tilde{\mathbf{h}}_{cp,k} \mathbf{x}_c \quad (4)$$

for $k \in \mathcal{K}$, where $\tilde{\mathbf{h}}_{pp,k} \triangleq s_{p,k}^* \mathbf{h}_{pp,k}$ and $\tilde{\mathbf{h}}_{cp,k} \triangleq s_{p,k}^* \mathbf{h}_{cp,k}$, and the corresponding SM constraints are given by

$$\delta_{p,k} = \mathcal{R}\{z_{p,k}\} \sin \theta - |\mathcal{I}\{z_{p,k}\}| \cos \theta \geq \delta_p^0, \forall k \in \mathcal{K}. \quad (5)$$

For any given complex vector \mathbf{x} , we define the operator

$$\mathcal{U}(\mathbf{x}) \triangleq \begin{bmatrix} \mathcal{R}\{\mathbf{x}\} \sin \theta - \mathcal{I}\{\mathbf{x}\} \cos \theta & -\mathcal{R}\{\mathbf{x}\} \cos \theta - \mathcal{I}\{\mathbf{x}\} \sin \theta \\ \mathcal{R}\{\mathbf{x}\} \sin \theta + \mathcal{I}\{\mathbf{x}\} \cos \theta & \mathcal{R}\{\mathbf{x}\} \cos \theta - \mathcal{I}\{\mathbf{x}\} \sin \theta \end{bmatrix} \quad (6)$$

and denote

$$\tilde{\mathbf{H}}_{pp,k}^{\mathcal{U}} = \mathcal{U}(\tilde{\mathbf{h}}_{pp,k}), \quad \tilde{\mathbf{H}}_{cp,k}^{\mathcal{U}} = \mathcal{U}(\tilde{\mathbf{h}}_{cp,k}). \quad (7)$$

Using the following real-valued notation,

$$\check{\mathbf{x}}_p = \begin{bmatrix} \mathcal{R}\{\mathbf{x}_p\} \\ \mathcal{I}\{\mathbf{x}_p\} \end{bmatrix}, \quad \check{\mathbf{x}}_c = \begin{bmatrix} \mathcal{R}\{\mathbf{x}_c\} \\ \mathcal{I}\{\mathbf{x}_c\} \end{bmatrix}, \quad (8)$$

the constraint in eq. (5) can be simplified as

$$\tilde{\mathbf{H}}_{pp,k}^{\mathcal{U}} \check{\mathbf{x}}_p + \tilde{\mathbf{H}}_{cp,k}^{\mathcal{U}} \check{\mathbf{x}}_c \geq \delta_p^0 \mathbf{1}_2 \quad \forall k \in \mathcal{K}. \quad (9)$$

Similarly, the rotated symbols at the CUs are

$$z_{c,j} = s_{c,j}^* r_{c,j} = \tilde{\mathbf{h}}_{cc,j} \mathbf{x}_c + \tilde{\mathbf{h}}_{pc,j} \mathbf{x}_p, \quad (10)$$

where $\tilde{\mathbf{h}}_{cc,j} \triangleq s_{c,j}^* \mathbf{h}_{cc,j}$, and $\tilde{\mathbf{h}}_{pc,j} \triangleq s_{c,j}^* \mathbf{h}_{pc,j}$, with SM constraints

$$\tilde{\mathbf{H}}_{cc,j}^{\mathcal{U}} \check{\mathbf{x}}_c + \tilde{\mathbf{H}}_{pc,j}^{\mathcal{U}} \check{\mathbf{x}}_p \geq \delta_c^0 \mathbf{1}_2 \quad \forall j \in \mathcal{J}. \quad (11)$$

Given the above, the general SLP power minimization problem with perfect CSI can be formulated as follows:

$$\underset{\check{\mathbf{x}}_c}{\text{minimize}} \quad \|\check{\mathbf{x}}_c\|^2 \quad (12)$$

$$\text{subject to} \quad \begin{bmatrix} -\tilde{\mathbf{H}}_{cp}^{\mathcal{U}} \\ -\tilde{\mathbf{H}}_{cc}^{\mathcal{U}} \end{bmatrix} \check{\mathbf{x}}_c \leq \begin{bmatrix} \tilde{\mathbf{H}}_{pp}^{\mathcal{U}} \\ \tilde{\mathbf{H}}_{pc}^{\mathcal{U}} \end{bmatrix} \check{\mathbf{x}}_p - \begin{bmatrix} \delta_p^0 \mathbf{1}_{2N_p} \\ \delta_c^0 \mathbf{1}_{2N_c} \end{bmatrix} \quad (13)$$

where $\tilde{\mathbf{H}}_{cp}^{\mathcal{U}} \triangleq \mathcal{U}(\text{diag}(\mathbf{s}_p^*)\mathbf{H}_{cp})$, $\tilde{\mathbf{H}}_{cc}^{\mathcal{U}} \triangleq \mathcal{U}(\text{diag}(\mathbf{s}_c^*)\mathbf{H}_{cc})$, $\tilde{\mathbf{H}}_{pp}^{\mathcal{U}} \triangleq \mathcal{U}(\text{diag}(\mathbf{s}_p^*)\mathbf{H}_{pp})$, and $\tilde{\mathbf{H}}_{pc}^{\mathcal{U}} \triangleq \mathcal{U}(\text{diag}(\mathbf{s}_c^*)\mathbf{H}_{pc})$. This is a quadratic programming problem with linear inequality constraints and can be efficiently solved.

4. ROBUST SLP FOR STOCHASTIC CSI ERRORS

For the case where the PBS CSI error is due to quantization, the quantized channels $\mathbf{h}_{pp,k}^Q$ and $\mathbf{h}_{pc,j}^Q$ shared by the PBS can be described using a statistical model such as AQNM [19, 20]. Here we assume the channels are Gaussian with zero mean and covariances given by $\mathbb{R}_{\mathbf{h}_{pp,k}} = \beta_p \mathbf{I}_{M_p}$ and $\mathbb{R}_{\mathbf{h}_{pc,j}} = \beta_c \mathbf{I}_{M_p}$. Using AQNM, the quantized CSI from the PBS after rotation is expressed as

$$\tilde{\mathbf{h}}_{pp,k}^Q = \mathbb{Q}(\tilde{\mathbf{h}}_{pp,k}) \approx \alpha_p \tilde{\mathbf{h}}_{pp,k} + \tilde{\mathbf{n}}_{pp,k}^Q \quad (14)$$

$$\tilde{\mathbf{h}}_{pc,j}^Q = \mathbb{Q}(\tilde{\mathbf{h}}_{pc,j}) \approx \alpha_c \tilde{\mathbf{h}}_{pc,j} + \tilde{\mathbf{n}}_{pc,j}^Q, \quad (15)$$

where $\mathbb{Q}(\cdot)$ is a scalar quantization function applied component-wise and separately to the real and imaginary parts. The vectors $\tilde{\mathbf{n}}_{pp,k}^Q \triangleq s_{p,k}^* \mathbf{n}_{pp,k}^Q$ and $\tilde{\mathbf{n}}_{pc,j}^Q \triangleq s_{c,j}^* \mathbf{n}_{pc,j}^Q$ denote the zero-mean Gaussian-distributed quantization noise vectors, and are assumed to be uncorrelated with $\tilde{\mathbf{h}}_{pp,k}$ and $\tilde{\mathbf{h}}_{pc,j}$. The scaling $\alpha = 1 - \rho$ is an attenuation factor based on the distortion $\rho = \frac{\mathbb{E}\{\|\mathbf{h} - \mathbf{h}^Q\|^2\}}{\mathbb{E}\{\|\mathbf{h}\|^2\}}$, which in turn depends on the bit resolution of the quantizer. For example, assuming an optimal non-uniform Lloyd-Max quantizer, the value of ρ is given in [21] for different bit resolutions b . The phase rotation does not alter the covariance matrices of the quantization noise, which are given by [19]

$$\mathbb{R}\{\tilde{\mathbf{n}}_{pp,k}^Q\} = \alpha_p \rho_p \beta_p \mathbf{I}_{M_p}, \quad \mathbb{R}\{\tilde{\mathbf{n}}_{pc,j}^Q\} = \alpha_c \rho_c \beta_c \mathbf{I}_{M_p}. \quad (16)$$

Based on eq. (14) and eq. (15), we can derive

$$\tilde{\mathbf{H}}_{pp,k}^{\mathcal{U}} = \bar{\alpha}_p (\tilde{\mathbf{H}}_{pp,k}^{Q,\mathcal{U}} - \tilde{\mathbf{N}}_{pp,k}^{Q,\mathcal{U}}) \quad (17)$$

$$\tilde{\mathbf{H}}_{pc,j}^{\mathcal{U}} = \bar{\alpha}_c (\tilde{\mathbf{H}}_{pc,j}^{Q,\mathcal{U}} - \tilde{\mathbf{N}}_{pc,j}^{Q,\mathcal{U}}), \quad (18)$$

where $\bar{\alpha}_p = \frac{1}{\alpha_p}$, $\bar{\alpha}_c = \frac{1}{\alpha_c}$, $\tilde{\mathbf{H}}_{pp,k}^{Q,\mathcal{U}} \triangleq \mathcal{U}(\tilde{\mathbf{h}}_{pp,k}^Q)$, $\tilde{\mathbf{N}}_{pp,k}^{Q,\mathcal{U}} \triangleq \mathcal{U}(\tilde{\mathbf{n}}_{pp,k}^Q)$, $\tilde{\mathbf{H}}_{pc,j}^{Q,\mathcal{U}} \triangleq \mathcal{U}(\tilde{\mathbf{h}}_{pc,j}^Q)$, and $\tilde{\mathbf{N}}_{pc,j}^{Q,\mathcal{U}} \triangleq \mathcal{U}(\tilde{\mathbf{n}}_{pc,j}^Q)$. Substituting eq. (17) and eq. (18) for (13), we have

$$\bar{\alpha}_p (\tilde{\mathbf{H}}_{pp,k}^{Q,\mathcal{U}} - \tilde{\mathbf{N}}_{pp,k}^{Q,\mathcal{U}}) \tilde{\mathbf{x}}_p + \tilde{\mathbf{H}}_{cp,k}^{\mathcal{U}} \tilde{\mathbf{x}}_c \geq \delta_p^0 \mathbf{1}_2, \quad \forall k \in \mathcal{K} \quad (19)$$

$$\tilde{\mathbf{H}}_{cc,j}^{\mathcal{U}} \tilde{\mathbf{x}}_c + \bar{\alpha}_c (\tilde{\mathbf{H}}_{pc,j}^{Q,\mathcal{U}} - \tilde{\mathbf{N}}_{pc,j}^{Q,\mathcal{U}}) \tilde{\mathbf{x}}_p \geq \delta_c \mathbf{1}_2, \quad \forall j \in \mathcal{J}. \quad (20)$$

The constraints above are expressed in terms of the unknown random quantization noise, and thus cannot be directly enforced. Instead, we choose to pose the problem such that the constraints are achieved with a certain probability. In particular, we rewrite (19) and (20) as follows:

$$\mathbb{P}\{\alpha_p \tilde{\mathbf{H}}_{cp,k}^{\mathcal{U}} \tilde{\mathbf{x}}_c + \tilde{\mathbf{H}}_{pp,k}^{Q,\mathcal{U}} \tilde{\mathbf{x}}_p - \alpha_p \delta_p^0 \mathbf{1}_2 \geq \tilde{\mathbf{N}}_{pp,k}^{Q,\mathcal{U}} \tilde{\mathbf{x}}_p\} \geq v_1 \quad (21)$$

$$\mathbb{P}\{\alpha_c \tilde{\mathbf{H}}_{cc,j}^{\mathcal{U}} \tilde{\mathbf{x}}_c + \tilde{\mathbf{H}}_{pc,j}^{Q,\mathcal{U}} \tilde{\mathbf{x}}_p - \alpha_c \delta_c \mathbf{1}_2 \geq \tilde{\mathbf{N}}_{pc,j}^{Q,\mathcal{U}} \tilde{\mathbf{x}}_p\} \geq v_2, \quad (22)$$

where $\mathbb{P}\{A\}$ denotes the probability of event A , and $\{v_1, v_2\} \in (0.5, 1]$ represent the probability thresholds. In the following two subsections, we find expressions for the probabilities in (21) and (22).

4.1. Primary System

It is easy to show that

$$\mathbb{E}\{\tilde{\mathbf{N}}_{pp,k}^{Q,\mathcal{U}}\} = \mathbf{0}_{2 \times 2M_p}, \quad \mathbb{R}_{\tilde{\mathbf{N}}_{pp,k}^{Q,\mathcal{U}}} = \alpha_p \rho_p \beta_p \mathbf{I}_{2M_p}, \quad (23)$$

$$\mathbb{E}\{\tilde{\mathbf{N}}_{pp,k}^{Q,\mathcal{U}} (\tilde{\mathbf{N}}_{pp,k}^{Q,\mathcal{U}})^H\} = M_p \alpha_p \rho_p \beta_p \begin{bmatrix} 1 & -\cos 2\theta \\ -\cos 2\theta & 1 \end{bmatrix} \quad (24)$$

The vector $\mathbf{q}_{p,k} \triangleq \tilde{\mathbf{N}}_{pp,k}^{Q,\mathcal{U}} \tilde{\mathbf{x}}_p \triangleq \begin{bmatrix} q_{p,k}^1 \\ q_{p,k}^2 \end{bmatrix}$ is a bivariate correlated Gaussian random vector with mean

$$\mathbb{E}\{\mathbf{q}_{p,k}\} = \mathbb{E}\{\tilde{\mathbf{N}}_{pp,k}^{Q,\mathcal{U}} \tilde{\mathbf{x}}_p\} = \mathbb{E}\{\tilde{\mathbf{N}}_{pp,k}^{Q,\mathcal{U}}\} \tilde{\mathbf{x}}_p = \mathbf{0}_{2 \times 1} \quad (25)$$

and covariance

$$\mathbb{R}_{\mathbf{q}_{p,k}} = \frac{P_p}{2} \alpha_p \rho_p \beta_p \begin{bmatrix} 1 & -\cos 2\theta \\ -\cos 2\theta & 1 \end{bmatrix}. \quad (26)$$

To simplify the notation, we define

$$\mathbf{w}_{p,k}(\tilde{\mathbf{x}}_c) \triangleq \alpha_p \tilde{\mathbf{H}}_{cp,k}^{\mathcal{U}} \tilde{\mathbf{x}}_c + \tilde{\mathbf{H}}_{pp,k}^{Q,\mathcal{U}} \tilde{\mathbf{x}}_p - \alpha_p \delta_p^0 \mathbf{1}_2 \triangleq \begin{bmatrix} w_{p,k}^1 \\ w_{p,k}^2 \end{bmatrix} \quad (27)$$

which is affine in $\tilde{\mathbf{x}}_c$. Using the new notation, the chance constraint (21) can be rewritten as

$$\mathbb{P}\{\mathbf{w}_{p,k}(\tilde{\mathbf{x}}_c) \geq \mathbf{q}_{p,k}\} \geq v_1. \quad (28)$$

No explicit closed-form expression for this probability seems possible, so we resort to a tractable approximation using the following lemma, whose proof can be found in [22].

Lemma 1. $\mathbb{P}\{\mathbf{w}_{p,k}(\tilde{\mathbf{x}}_c) \geq \mathbf{q}_{p,k}\} \geq v_1$ can be approximated by the inequality

$$\alpha_p \tilde{\mathbf{H}}_{cp,k}^{\mathcal{U}} \tilde{\mathbf{x}}_c + \tilde{\mathbf{H}}_{pp,k}^{Q,\mathcal{U}} \tilde{\mathbf{x}}_p \geq \eta_p \mathbb{R}_{\mathbf{q}_{p,k}}^{\frac{1}{2}} \mathbf{1}_2 + \alpha_p \delta_p^0 \mathbf{1}_2 \quad (29)$$

where $\eta \triangleq \sqrt{2} \operatorname{erf}^{-1}(2\sqrt{v_1} - 1)$.

4.2. Cognitive System

The constraint in (22) for the cognitive system can be found in an identical fashion. We define

$$\mathbf{q}_{c,j} \triangleq \tilde{\mathbf{N}}_{pc,j}^{Q,\mathcal{U}} \tilde{\mathbf{x}}_p \triangleq \begin{bmatrix} q_{c,j}^1 \\ q_{c,j}^2 \end{bmatrix}$$

$$\mathbf{w}_{c,j}(\tilde{\mathbf{x}}_c) \triangleq \alpha_c \tilde{\mathbf{H}}_{cc,j}^{\mathcal{U}} \tilde{\mathbf{x}}_c + \tilde{\mathbf{H}}_{pc,j}^{Q,\mathcal{U}} \tilde{\mathbf{x}}_p - \alpha_c \delta_c \mathbf{1}_2 \triangleq \begin{bmatrix} w_{c,j}^1 \\ w_{c,j}^2 \end{bmatrix},$$

which is affine in $\tilde{\mathbf{x}}_c$. Using the new notation, the constraint (22) can be rewritten as $\mathbb{P}\{\mathbf{w}_{c,j}(\tilde{\mathbf{x}}_c) \geq \mathbf{q}_{c,j}\} \geq v_2$. Like the technique used for the primary system, we define $\tilde{\mathbf{w}}_{c,j}(\tilde{\mathbf{x}}_c) \triangleq \mathbb{R}_{\mathbf{q}_{c,j}}^{-\frac{1}{2}} \mathbf{w}_{c,j}(\tilde{\mathbf{x}}_c)$ and $\bar{\mathbf{q}}_{c,j} \triangleq \mathbb{R}_{\mathbf{q}_{c,j}}^{-\frac{1}{2}} \mathbf{q}_{c,j}$. The following lemma, whose proof is identical to that of Lemma 1, can be obtained.

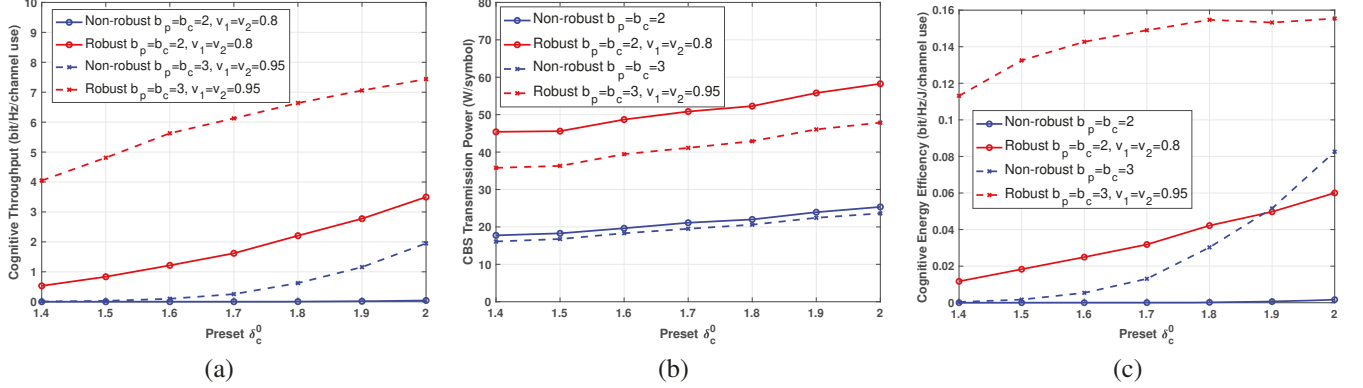


Fig. 2. (a) Throughput of CUs; (b) Transmit Power at CBS; (c) EE at CBS vs. SM at the CUs.

Lemma 2. $\mathbb{P}\{\bar{\mathbf{w}}_{c,j}(\check{\mathbf{x}}_c) \geq \bar{\mathbf{q}}_{c,j}\} \geq v_2$ can be approximated by the inequality

$$\alpha_c \tilde{\mathbf{H}}_{cc,j}^{\mathcal{V}} \check{\mathbf{x}}_c + \tilde{\mathbf{H}}_{pc,j}^{Q,\mathcal{V}} \check{\mathbf{x}}_p \geq \eta_c \mathbb{R}_{\mathbf{q}_{c,j}}^{\frac{1}{2}} \mathbf{1}_2 + \alpha_c \delta_c \mathbf{1}_2, \quad (30)$$

where $\eta_c = \sqrt{2} \operatorname{erf}^{-1}(2\sqrt{v_2} - 1)$ is a preset constant.

4.3. Robust SLP Design

We can now formulate the robust SLP algorithm with the probabilistic constraints below, which again is a quadratic program with linear inequality constraints.

$$\begin{aligned} & \underset{\check{\mathbf{x}}_c}{\text{minimize}} \quad \|\check{\mathbf{x}}_c\|^2 \\ & \text{subject to} \quad \alpha_p \tilde{\mathbf{H}}_{cp,k}^{\mathcal{V}} \check{\mathbf{x}}_c + \tilde{\mathbf{H}}_{pp,k}^{Q,\mathcal{V}} \check{\mathbf{x}}_p \geq \eta_p \mathbb{R}_{\mathbf{q}_{p,k}}^{\frac{1}{2}} \mathbf{1}_2 + \alpha_p \delta_p \mathbf{1}_2 \\ & \quad \alpha_c \tilde{\mathbf{H}}_{cc,j}^{\mathcal{V}} \check{\mathbf{x}}_c + \tilde{\mathbf{H}}_{pc,j}^{Q,\mathcal{V}} \check{\mathbf{x}}_p \geq \eta_c \mathbb{R}_{\mathbf{q}_{c,j}}^{\frac{1}{2}} \mathbf{1}_2 + \alpha_c \delta_c \mathbf{1}_2, \\ & \quad \forall k \in \mathcal{K} \text{ and } \forall j \in \mathcal{J}. \end{aligned} \quad (31)$$

5. NUMERICAL RESULTS

In this section, we assess the performance of our proposed power-minimizing SLP (PMSLP) approach. Monte-Carlo simulations are conducted over 1000 independent channel realizations with a block of $T = 100$ symbols. The channels \mathbf{H}_{pp} , \mathbf{H}_{cp} , \mathbf{H}_{pc} and \mathbf{H}_{cc} are composed of i.i.d. Gaussian random variables with zero mean and unit variance, and the PBS channel is assumed to be quantized using an optimal non-uniform Lloyd-Max quantizer [21]. The complex Gaussian noise is assumed to have the same power ($\sigma_p = \sigma_c = 1$) for all PUs and CUs. The PBS transmission power is $P_p = 10$ dBW. Both the PBS and CBS are assumed to have $M_p = M_c = 8$ antennas and the number of PUs and CUs are both set at $N_p = N_c = 4$. The preset SM at the PUs is $\delta_p^0 = 1.5$. We further assume zero-forcing precoding at the PBS and QPSK modulation. We use energy efficiency (EE) to quantify the power-performance trade-off between the robust and non-robust designs, which is defined as the ratio

between the throughput τ [23] and the transmit power per channel, i.e., $\text{EE} = \frac{\tau}{T \times \|\check{\mathbf{x}}_c\|^2}$.

Fig. 2(a) shows the throughput of the CUs as a function of the SM threshold at the CUs (δ_c^0), assuming either $b = 2$ or $b = 3$ quantization bits per channel coefficient and different probability constraints. We see that the CUs reap benefits from the robust SLP design, achieving significantly higher throughput. However, in Fig. 2(b) we see that as the preset δ_c^0 increases, the CBS with robust SLP requires more power to meet the SM constraint than the non-robust SLP. For a fair comparison, we plot the EE at the CBS in Fig. 2(c). It is clear that the larger the SM or the higher the quantization resolution, the higher the EE. When $b = 3$, $\delta_c^0 = 1.7$, the EE of the robust SLP is approximately 10 times greater than that of the non-robust SLP. To quantify the performance gain that comes from the interference exploitation, we also implemented a block level precoding method like ZF method in [5], and found that a safety margin greater than 1 could only be obtained when the transmit power is greater than 200 W/symbol. Moreover, unlike the proposed approach, the throughput and EE is near 0 in this scenario.

6. CONCLUSION

In this paper, we designed a robust SLP algorithm for overlay CR systems with the goal to minimize the CBS transmit power and simultaneously ensure the QoS (here, the SM) of both the PUs and CUs. Unlike traditional precoding techniques, we use SM constraints instead of SINR or BER metrics in order to exploit CI. With the CSI error described using AQNM, we construct a probability-constrained problem and derive an approximate deterministic formulation. The numerical results demonstrate that our robust SLP scheme can effectively deal with quantized CSI to maintain an acceptable QoS at both the PUs and CUs.

7. REFERENCES

- [1] I. F. Akyildiz, W. Y. Lee, M. C. Vuran, and S. Mohanty, “NeXt generation/dynamic spectrum access/cognitive radio wireless networks: A survey,” *Comput. Netw.*, vol. 50, no. 13, pp. 2127–2159, Sept. 2006.
- [2] A. Goldsmith, S. A. Jafar, I. Maric, and S. Srinivasa, “Breaking spectrum gridlock with cognitive radios: An information theoretic perspective,” *Proc. IEEE*, vol. 97, no. 5, pp. 894–914, Apr. 2009.
- [3] W. Liang, S. X. Ng, and L. Hanzo, “Cooperative overlay spectrum access in cognitive radio networks,” *IEEE Commun. Surveys Tuts.*, vol. 19, no. 3, pp. 1924–1944, 2017.
- [4] C. Masouros, “Correlation rotation linear precoding for MIMO broadcast communications,” *IEEE Trans. Signal Process.*, vol. 59, no. 1, pp. 252–262, Oct. 2010.
- [5] F. A. Khan, C. Masouros, and T. Ratnarajah, “Interference-driven linear precoding in multiuser miso downlink cognitive radio network,” *IEEE Trans. Veh. Technol.*, vol. 61, no. 6, pp. 2531–2543, 2012.
- [6] C. Masouros and G. Zheng, “Exploiting known interference as green signal power for downlink beamforming optimization,” *IEEE Trans. Signal Process.*, vol. 63, no. 14, pp. 3628–3640, May 2015.
- [7] H. Jedda, A. Mezghani, A. Swindlehurst, and J. A. Nossek, “Quantized constant envelope precoding with PSK and QAM signaling,” *IEEE Trans. Wireless Commun.*, vol. 17, no. 12, pp. 8022–8034, Oct. 2018.
- [8] A. Haqiqatnejad, F. Kayhan, and B. Ottersten, “Symbol-level precoding design based on distance preserving constructive interference regions,” *IEEE Trans. Signal Process.*, vol. 66, no. 22, pp. 5817–5832, Oct. 2018.
- [9] A. Li, C. Masouros, B. Vucetic, Y. Li, and A. Swindlehurst, “Interference exploitation precoding for multi-level modulations: Closed-form solutions,” *IEEE Trans. Commun.*, vol. 69, no. 1, pp. 291–308, Oct. 2021.
- [10] N. Jindal, “MIMO broadcast channels with finite-rate feedback,” *IEEE Trans. Inf. Theory*, vol. 52, no. 11, pp. 5045–5060, Oct. 2006.
- [11] B. K. Chalise, S. Shahbazpanahi, A. Czylwik, and A. B. Gershman, “Robust downlink beamforming based on outage probability specifications,” *IEEE Trans. Wireless Commun.*, vol. 6, no. 10, pp. 3498–3503, Oct. 2007.
- [12] N. Vucic and H. Boche, “Robust QoS-constrained optimization of downlink multiuser MISO systems,” *IEEE Trans. Signal Process.*, vol. 57, no. 2, pp. 714–725, Oct. 2008.
- [13] G. Zheng, K. K. Wong, and B. Ottersten, “Robust cognitive beamforming with bounded channel uncertainties,” *IEEE Trans. Signal Process.*, vol. 57, no. 12, pp. 4871–4881, July 2009.
- [14] G. Zheng, S. Ma, K. K. Wong, and T. S. Ng, “Robust beamforming in cognitive radio,” *IEEE Trans. Wireless Commun.*, vol. 9, no. 2, pp. 570–576, Feb. 2010.
- [15] S. Ma and D. Sun, “Chance constrained robust beamforming in cognitive radio networks,” *IEEE Commun. Lett.*, vol. 17, no. 1, pp. 67–70, Nov. 2012.
- [16] I. Wajid, M. Pesavento, Y. C. Eldar, and D. Ciochino, “Robust downlink beamforming with partial channel state information for conventional and cognitive radio networks,” *IEEE Trans. Signal Process.*, vol. 61, no. 14, pp. 3656–3670, May 2013.
- [17] A. Haqiqatnejad, S. Shahbazpanahi, and B. Ottersten, “A worst-case performance optimization based design approach to robust symbol-level precoding for downlink MU-MIMO,” in *Proc. IEEE Glob. Conf. on Signal and Inf. Process. (GlobalSIP)*, Jan. 2019, pp. 1–5.
- [18] A. Haqiqatnejad, F. Kayhan, and B. Ottersten, “Robust SINR-constrained symbol-level multiuser precoding with imperfect channel knowledge,” *IEEE Trans. Signal Process.*, vol. 68, pp. 1837–1852, Mar. 2020.
- [19] Q. Bai, A. Mezghani, and J. A. Nossek, “On the optimization of ADC resolution in multi-antenna systems,” in *Proc. Int. Symp. on Wireless Commun. Syst. (ISWCS)*, Aug. 2013, pp. 1–5.
- [20] Q. Bai and J. A. Nossek, “Energy efficiency maximization for 5G multi-antenna receivers,” *Trans. Emerg. Telecommun. Technol.*, vol. 26, no. 1, pp. 3–14, Jan. 2015.
- [21] J. Max, “Quantizing for minimum distortion,” *IEEE Trans. Inf. Theory*, vol. 6, no. 1, pp. 7–12, Mar. 1960.
- [22] L. Liu, C. Masouros, and A. Swindlehurst, “Robust symbol level precoding for overlay cognitive radio networks,” <http://arxiv.org/abs/2301.08393/>, 2023.
- [23] A. Salem and C. Masouros, “Error probability analysis and power allocation for interference exploitation over Rayleigh fading channels,” *IEEE Trans. Wireless Commun.*, Apr. 2021.